Communication in Physical Sciences 2025, 12(5): 1442-1455

Effect of Cerium on the Dielectric and Structural Properties of Barium Titanate-based Ceramics for Multilayer Ceramic Capacitors

Lariski F M[1] and Hassan Abdulsalam*
Received: 27 May 2025/Accepted: 25 June 2025/Published: 01 July 2025
https://dx.doi.org/10.4314/cps.v12i5.1

Abstract: *Cerium-doped $BaTi_{1-x}Ce_xO_3$ (x = 0.0, 0.15, 0.25) ceramics were synthesized using the sol-gel auto-combustion technique. An appropriate amount of the chemicals was dissolved in 100ml of distilled water in stoichiometric ratios to form an aqueous solution. The fine barium titanate precursor was pre-calcinated in a digitally controlled muffle furnace at 900°C for 5h. X-ray diffraction (XRD) pattern of the samples indicates that the calcined samples present the formation of a tetragonal crystal structure of $BaTiO_3$. The diffraction peaks tend to have cubic symmetry due to Ce doping. The unit cell volume increases rapidly due to Ce doping This is attributed to the substitution of Ce ions at Ti sites, Fourier Transform Infrared Spectroscopy (FTIR) shows a strong absorption peak for pure BT powder is obtained at $484cm^{-1}$, $485cm^{-1}$ and $487cm^{-1}$ for (x = 0.0, 0.15, 0.25) respectively, hence the bond energy increases with increase in doping concentration. The Field Emission Scanning Electron Microscopy (FESEM) and Energy Dispersive Spectroscopy (EDX) prepared at 1,100 °C for 5 h show a homogeneous particle size of about 50.77nm and 75.87nm for x = 0.00 and 0.25, respectively. With Ce doping, a more homogeneous grain size evolved with an increase in average grain size and density with an increase in Ce doping concentration. The EDX spectra show the presence of Ba, Ti, Ce, and O. The result confirms that pure barium titanate is a dominant phase. There is an enhancement in the dielectric constant in the sample with the highest amount of Cerium (x= 0.25) characteristic of the copper sample, which is a good material for Multilayer ceramic capacitors.*

Keywords*: Barium titanate; Lattice Constant; Morphology; Dielectric constant; Ceramics*

Fatima Musa Lariski
Department of Physics, Faculty of Science, Yobe State University, Damaturu, Yobe State, Nigeria
Email: habdulsalam@ysu.edu.ng
Orcid id: 0000-0003-4271-3597

Hassan Abdulsalam*
Department of Physics, Faculty of Science, Yobe State University, Damaturu, Yobe State, Nigeria
Email: fmusalariski@gmail.com

1.0 Introduction

Rare earth oxides (REOs) and metals are a significant class of materials that have sparked interest in modern technology worldwide. REOs and metals (which include Yb, Er, Sm, Eu, Y, Gd, Dy, and Ce) are primarily used in various chemical and industrial sectors and can improve the dielectric properties of barium titanate ($BaTiO_3$)-based ceramics (Hossain *et al.*, 2022; Zhang *et al.*, 2020). Stoichiometric double doping can accelerate the dissolution of a rare-earth element, as each dopant is more soluble due to essentially no ionic defects(A. Kumari & Ghosh, 2018). It has been found that adding a small amount of RE to $BaTiO_3$ compounds significantly improves their mechanical, dielectric, and synthesis properties, as well as their microstructure and phase structure, while also lowering the transition temperature(Alshoaibi *et al.*, 2020; Ismail *et al.*, 2016).

Despite these advancements, there remains a lack of comprehensive understanding regarding the B-site vacancy compensation

model in RE-doped $BaTiO_3$ ceramics. This study specifically addresses this knowledge gap by investigating the structural and dielectric behaviour of Ce^{4+}-Ce^{4}-substituted $BaTiO_3$, where Ce^{4+} replaces Ti^{4+} in the perovskite lattice. Cerium is particularly interesting due to its ability to stabilize the cubic phase near room temperature, which enhances the material's dielectric tunability and thermal stability; both critical for multilayer ceramic capacitor (MLCC) applications (Y.-M. Zhang *et al.*, 2006; Hwang & Han, 2001).

Cerium greatly lowers the Curie temperature of $BaTiO_3$, making cerium-doped dielectric ceramics of practical interest (Cernea *et al.*, 2006). Due to its excellent dielectric, ferroelectric properties and low loss characteristics, $BaTiO_3$ with a perovskite structure, generalized as $A^{2+}B^{4+}O^{3-}$, is the most widely used ferroelectric material. It is extensively employed in capacitors and electronic devices such as smartphones, personal computers, and passive components(Kim *et al.*, 2012; Kumari *et al.*, 2015; Sharma *et al.*, 2020).

Over the past few decades, doping $BaTiO_3$ with RE elements has become a growing field of study(Ganguly *et al.*, 2013). Doping with mid-to-heavy rare-earth elements like Y, Dy, and Ho has proven effective at extending the lifespan of ceramic components(Itoh *et al.*, 2002). Several studies have examined the impact of rare-earth doping, particularly partial substitutions of tetravalent Ce ions for Ti sites, on the dielectric characteristics of $BaTiO_3$ (Lu *et al.*, 2005).

Cerium is a unique RE element with an electronic configuration of $4f^1$ $5d^1$ $6s^2$, allowing it to substitute for Ti ions in $BaTiO_3$ (Y.-M. Zhang *et al.*, 2006). Its ability to switch between valence states (Ce^{3+} and Ce^{4+}) makes it attractive for defect engineering. The ionic radii suggest that Ce^{3+} exchanges with the dodecahedral coordinated A-site, whereas Ce^{4+} enters the octahedrally coordinated B-site. Ce^{4+}, being more stable than Ce^{3+}, is generally preferred(Zhao *et al.*, 2020). The valence and ionic radius of replacing ions determine whether doping occurs at the A or B site (Joshi *et al.*, 2014; Petrović *et al.*, 2015). It has been observed that Ce^{3+} substitution at Ba^{2+} sites consistently lowers the Curie temperature (Tc) of $BaTiO_3$, whereas Ce^{4+} substitution at Ti^{4+} sites has minimal effect on Tc. Thus, Ce can act as a substitute for both Ba and Ti sites depending on the Ba/Ti ratio (Hwang & Han, 2001). On Earth's crust, Ce is the most abundant rare-earth element; more prevalent than copper (Alam *et al.*, 2012).

Structural modifications are typically pursued for two reasons: (1) to raise permittivity and (2) to increase frequency-temperature and dielectric stability close to room temperature (Zhang *et al.*, 2006). Defects significantly impact the dielectric characteristics of $BaTiO_3$-based devices. To reduce electric conductivity induced by defects, various bivalent or trivalent elements have been utilized to replace Ti for charge compensation (Joshi *et al.*, 2014). $BaTiO_3$ is among the most common ceramic materials used for electronic purposes (A. Kumari & Ghosh, 2018).

By adjusting the doping quantity of appropriate rare-earth ions, it is possible to produce ferroelectric materials with a reasonable dielectric constant and minimal dielectric loss (Kim *et al.*, 2012; Kumari *et al.*, 2015). The production of MLCCs with high capacitances using Ce-modified $BaTiO_3$ offers significant advantages, including enhanced flexural strength, excellent DC bias characteristics, and a tunable dielectric constant–temperature relationship controllable via Ce doping levels (Y.-M. Zhang *et al.*, 2006; Kim *et al.*, 2012).

Studies have shown that Ce doping enhances the dielectric constant while maintaining low dielectric loss (tan δ) at low frequencies, essential for minimizing energy dissipation and ensuring efficient capacitor performance(Beena & Jayanna, 2019; Arshad

et al., 2020). Moreover, Ce substitution at Ti sites stabilizes the crystal structure and reduces the tetragonality of $BaTiO_3$, promoting a cubic-to-tetragonal phase transition near room temperature. This allows for better temperature stability and improved dielectric tunability, both critical for MLCC applications(Zhang *et al.*, 2006).

Additionally, Ce doping leads to a more homogeneous microstructure with increased grain size and density, as evidenced by FESEM analysis, which contributes to improved mechanical integrity and reduced leakage currents(Mitic *et al.*, 2010). The observed increase in bond energy—as indicated by FTIR peak shifts—further supports greater thermal and chemical stability, making Ce-doped $BaTiO_3$suitable for use in harsh environments(Kim *et al.*, 2012).

The combination of high dielectric constant, low loss, controlled temperature dependence, and improved structural and electrical properties makes Ce-modified $BaTiO_3$ a highly suitable material for next-generation MLCCs requiring miniaturisation, high performance, and long-term reliability.

The main purpose of this research is the synthesis and characterization of B-site deficient Ce rare-earth doped $BaTiO_3$ with chemical compositions $BaTi_{1-x}Ce_xO_3$ ($x = 0.0, 0.15, 0.25$). In this paper, we study the role of an individual Ce dopant on the structural and morphological properties of $BaTiO_3$-based ceramics.

2.0 Materials and Methods

2.1 Chemicals and Reagents

The chemicals and reagents used are high-purity (99%–99.5%) analytical reagents (AR grade). The chemicals include barium nitrate [Ba $(NO_3)_2$] (Loba Chemie), titanium dioxide (TiO_2) (Loba Chemie), cerium nitrate [Ce $(NO_3)_2$] (CDH), citric acid ($C_6H_8O_7$) (Loba Chemie), with distilled water as the solvent. All the chemicals and reagents were used as received without any further purification.

2.2 Experimental Details

Synthesis of Ce^{4+} substituted $BaTiO_3$ with chemical composition $BaTi_{1-x}Ce_xO_3$ ($x = 0.0, 0.15, 0.25$) has been successfully synthesized using sol-gel technique. An appropriate amount of the chemicals was dissolved in 100ml of distilled water in stoichiometric ratios to form an aqueous solution. The molar ratio of citric acid to cation was maintained at 1:2. The prepared solution was heated at a temperature of 80–100°C. The solution was stirred using constant and continuous magnetic stirring in order to evaporate the water; a white gel was obtained, which was transferred to a hot plate and heated at a temperature of 280–300 °C. This gives a black precursor material which was ground with a mortar and pestle to obtain a fine barium titanate precursor which was precalcinated in a digitally controlled muffle furnace at 900°C for 5 h. The pre-calcinated powder was divided into three parts and labelled MA1, MA2, and MA3. Furthermore, MA1, MA2 and MA3 were further heated at 1100°C for 5 h. The obtained product was crushed using a mortar and pestle to obtain the fine barium titanate ceramic powder, followed by various characterizations.

2.3 Characterization

Structural and phase analysis were carried out with a Bruker AXS D8 advanced XRD diffractometer. Functional groups were also evaluated from FTIR spectra obtained with a Nicolet FTIR interferometer infrared Prestige-21 (model 8400S). The morphology and elemental analysis were studied using FESEM/energy-dispersive X-ray (EDX) spectroscopy (FEI Nova NanoSEM 450 FE-SEM) at a voltage of 15KV.

3.0 Results and discussion

3.1 XRD analysis

The XRD patterns of $BaTi_{1-x}Ce_xO_3$ ($x = 0.0, 0.15, 0.25$) are shown in Fig. 1. The diffraction peaks observed were indexed using JCPDS card number 79-2263 (Hai *et al.*, 2014). The calcined samples present the

formation of the tetragonal crystal structure of $BaTiO_3$. Because of the doping of Ce, the diffraction peaks frequently exhibit cubic symmetry. As evidenced by the quick rise in unit cell volume caused by Ce doping (Table 1). This is attributed to the replacement of Ce ions at Ti sites because the skeleton of a perovskite structure is made up of TiO, octahedra, and the 6-coordinate Ce^{4+} ionic radius (0.087 Å) is larger than the Ti^{4+} ionic radius (0.0605 Å). (Chemistry, 2006). The lattice constant (a) and the volume of the unit cell (V_{cell}) were calculated using Equations (1) and (2).

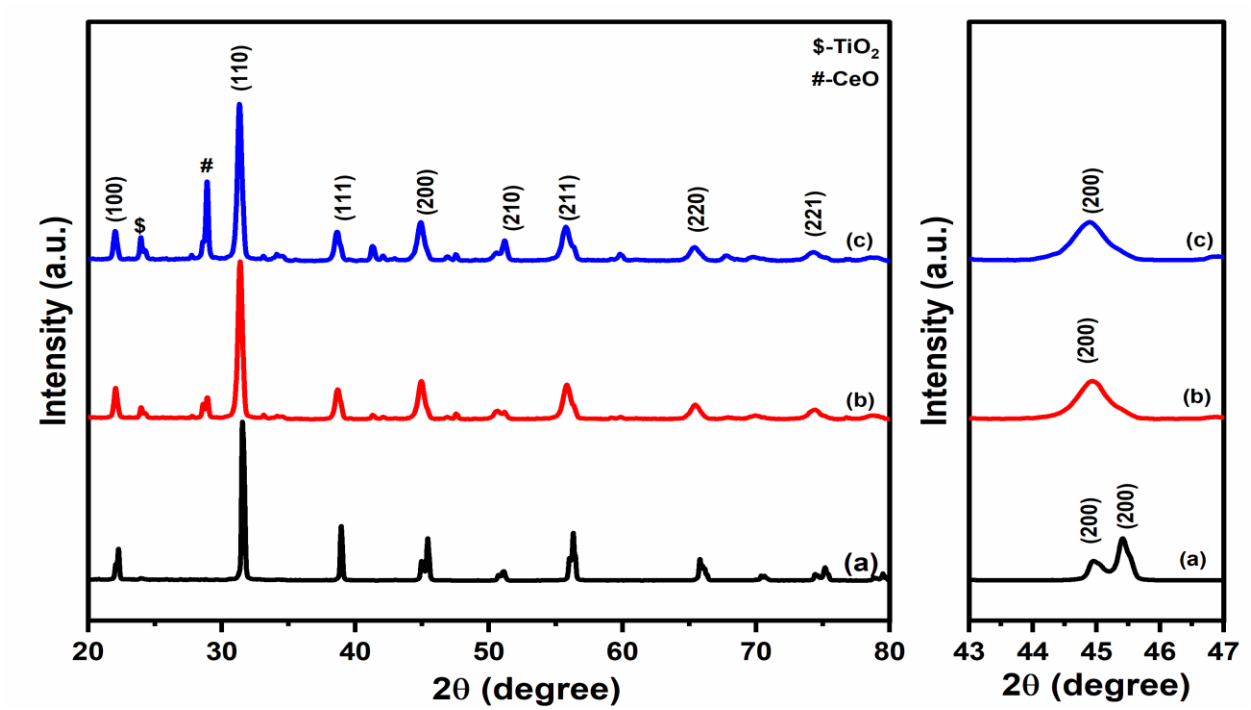
$$a = d\sqrt{h^2 + k^2 + l^2} \quad (1)$$

$$V_{cell} = a^3 \quad (2)$$

where d is the interplanar spacing, h, k and l are the Miller indices. The lattice constant, the interplanar spacing and the volume of the unit cell are shown in Table 1. From the calculated table, it was found that the lattice constant increases with an increase in Ti-Ce concentrations, likewise, the volume of the unit cell increases with an increase in Ti-Ce concentrations. We assume the lattice grows when rare earth ions (RE) are present on the B-site and contracts when RE are present on the A-site and when there are vacancies(Tsur *et al.*, 2001).

Table 1: Lattice Parameters and Unit Cell Volume of Ba (Ti $_{1-x}$ Ce$_x$) O$_3$ for (hkl) = (110)

x	0.00	0.15	0.25
d (Å)	2.8232	2.8234	2.8238
a (Å)	3.9926	3.9928	3.9934
v_{cell} (Å^3)	63.6454	63.6550	63.6837



Fig, 1: XRD patterns of BaTi1-xCexO3 (x = 0.0, 0.15, 0.25)

The spectra indicate the predominant presence of doped perovskite cubic phase with a cell parameter of 3.9926 Å and space group P4mm, for (110) Miller indices. Since the radius of the Ce ion is bigger than titanium, when cerium is incorporated at the B-site, a more closely packed BO_6 octahedral is achieved with enhanced thermal stability. Although this doping causes structural distortion, it also results in a decrease in the oxygen octahedron

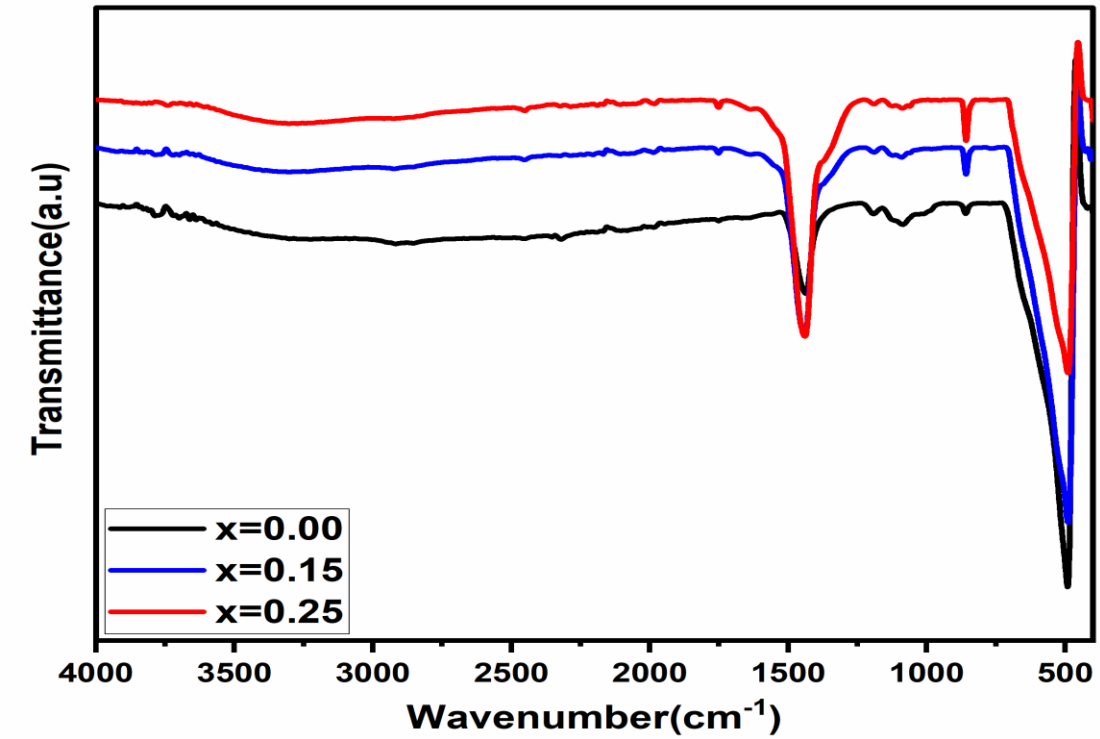
interstices, which strengthens the octahedra (Ganguly *et al.*, 2013). The existence of the RE element in the powder is shown by the peak's inclusion in the XRD spectra. Ion replacement with $BaTiO_3$ causes the second phase to coincide. (Joshi et al., 2015). The expansion of sites with larger Ce ions in the $BaTiO_3$ host lattice, as shown in Fig. 1 ($, and #), is responsible for the large XRD peaks shifts to the low angle of BaTiO3, demonstrating that Ce doping causes a larger lattice strain and further destroys the long-range order of the $BaTiO_3$ lattice. as reported by (Lu *et al.*, 2007). The charge balance compensation mechanism may be described as follows:

$$BaO + CeO_2 \rightarrow Ba_{Ba} + CeTi + 3O_2$$

The impurities in the starting materials and the defects are composed of Ce^{4+} ions at the Ti sites (CeTi)

3.2 FTIR analysis

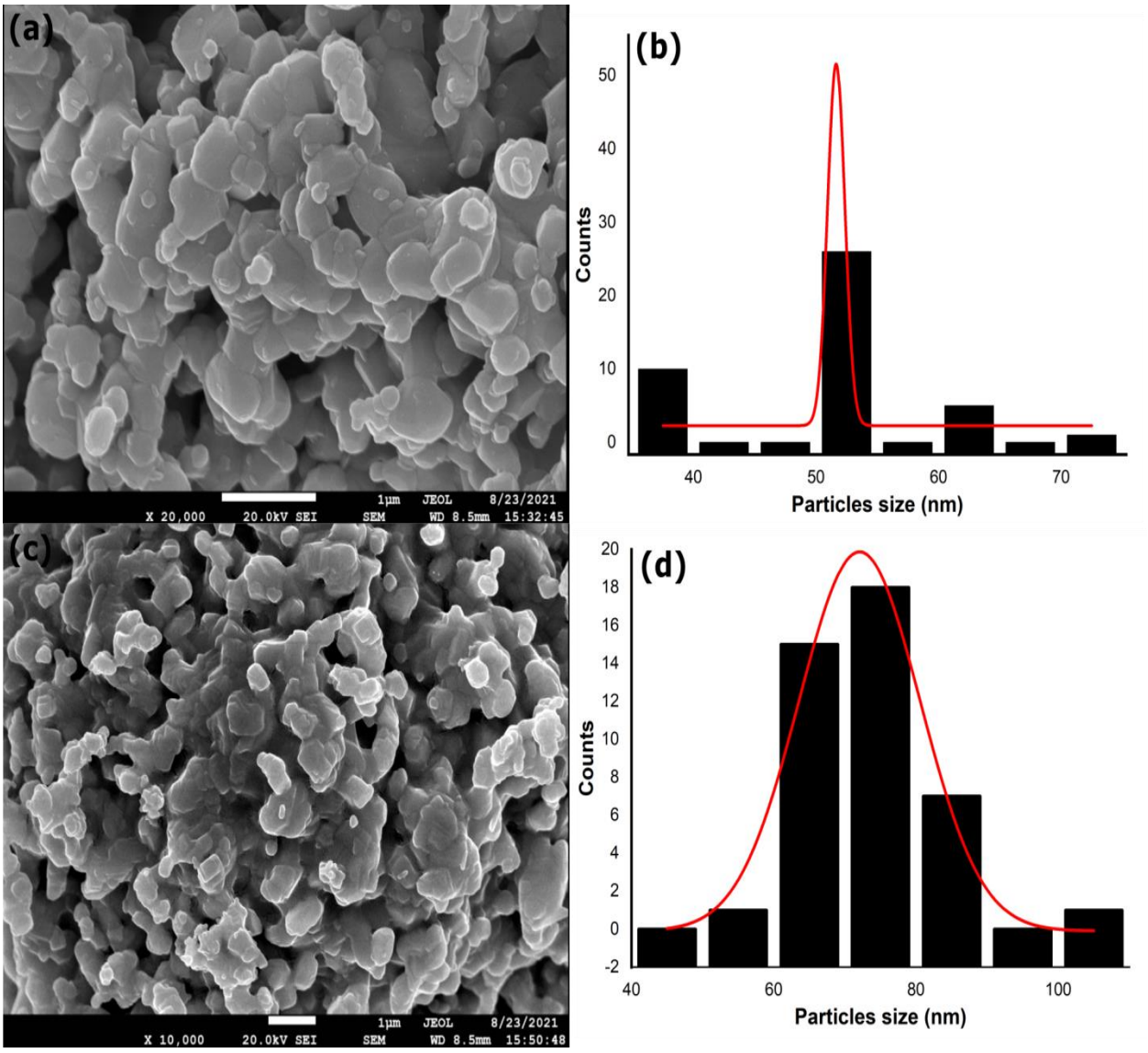
Fig 2 shows the FTIR spectra of $BaTi_{1-x}Ce_xO_3$ (x = 0.0, 0.15, 0.25) in the wave number range 500-4000 cm^{-1}. To examine the impact of additions in the ceramic, the FTIR method was used. FTIR is a useful tool to investigate the relationship between the physical characteristics and microstructure of perovskite ferroelectric materials since the ferroelectricity in these materials is highly dependent on the vibration of the crystal lattice. Due to its sensitivity to chemical bonding, FTIR is a crucial technology for studying the reaction process used in the creation of materials. (Kumari & Ghosh, 2018). A strong absorption peak for pure BT powder is obtained at 484cm^{-1}, 485cm^{-1} and 487cm^{-1} for (x = 0.0, 0.15, 0.25), respectively. This mode is crucial because the spontaneous polarization in BT with the tetragonal phase runs parallel to the direction of stretched normal vibration, as seen in (Ganguly, Rout, Park, et al., 2013). Another peak is observed at 1424cm^{-1}, 1436cm^{-1}, and 1445cm^{-1} for (x = 0.0, 0.15, 0.25), respectively. A shift of absorption peaks for the stretching normal vibration of Ti-O octahedron towards higher energy is observed. Hence, the bond energy increases with an increase in doping concentration.



Fig, 2: FTIR spectra of BaTi1-xCexO3 (x = 0.0, 0.15, 0.25)

3.3 FESEM analysis

FESEM and EDS were used to analyze the material's surface morphology (Hossain *et al.*, 2022) Fig, 3 (a) and (c) show the field emission scanning electron microscopy micrographs of the sample $BaTi_{1-x}Ce_xO_3$ (x = 0.0 and 0.25), prepared at 1,100 ^oC for 5 h. The fired powders of (Ba, Ce) TiO_3 solid solution show homogeneous particle sizes of about 50.77nm and 75.87nm for x = 0.00 and 0.25, respectively. With Ce doping, a more homogeneous grain size evolved with an increase in average grain size and density with an increase in doping concentration. Neither any kind of microcrack nor any kind of pore is identified anywhere, as reported by (Ganguly, Rout, et al., 2013)



Fig, 3: FESEM micrograph and particle distribution of BaTi1-xCexO3 (x = 0.00, and 0.25).

It is clearly evident that all pellets are highly dense, Ce-doped polycrystalline ceramics have larger grain sizes than undoped polycrystalline ceramics (Zhong *et al.*, 2005). The pure $BaTiO_3$ ceramics were not uniform in grain size distribution and some large grains were observed, which can affect the electric properties of $BaTiO_3$ ceramics strongly (Joshi

et al., 2014). Though it was reported that in some instances $BaTi_{1-x}Ce_xO_3$ ceramics show an inhomogeneous grain size distribution (Zhang *et al.*, 2006). Also Morphological tudy shows that the addition of rare-earth ions affects the growth of the grain and remarkably changes the grain morphology as reported by (Feng *et al.*, 2012). With the doping of additives, the grains became smaller, the density became higher, and the cracks and pores accumulation gradually disappeared. The EDX spectra show the presence of Ba, Ti, Ce, and O. The result confirms that pure barium titanate is a dominant phase.

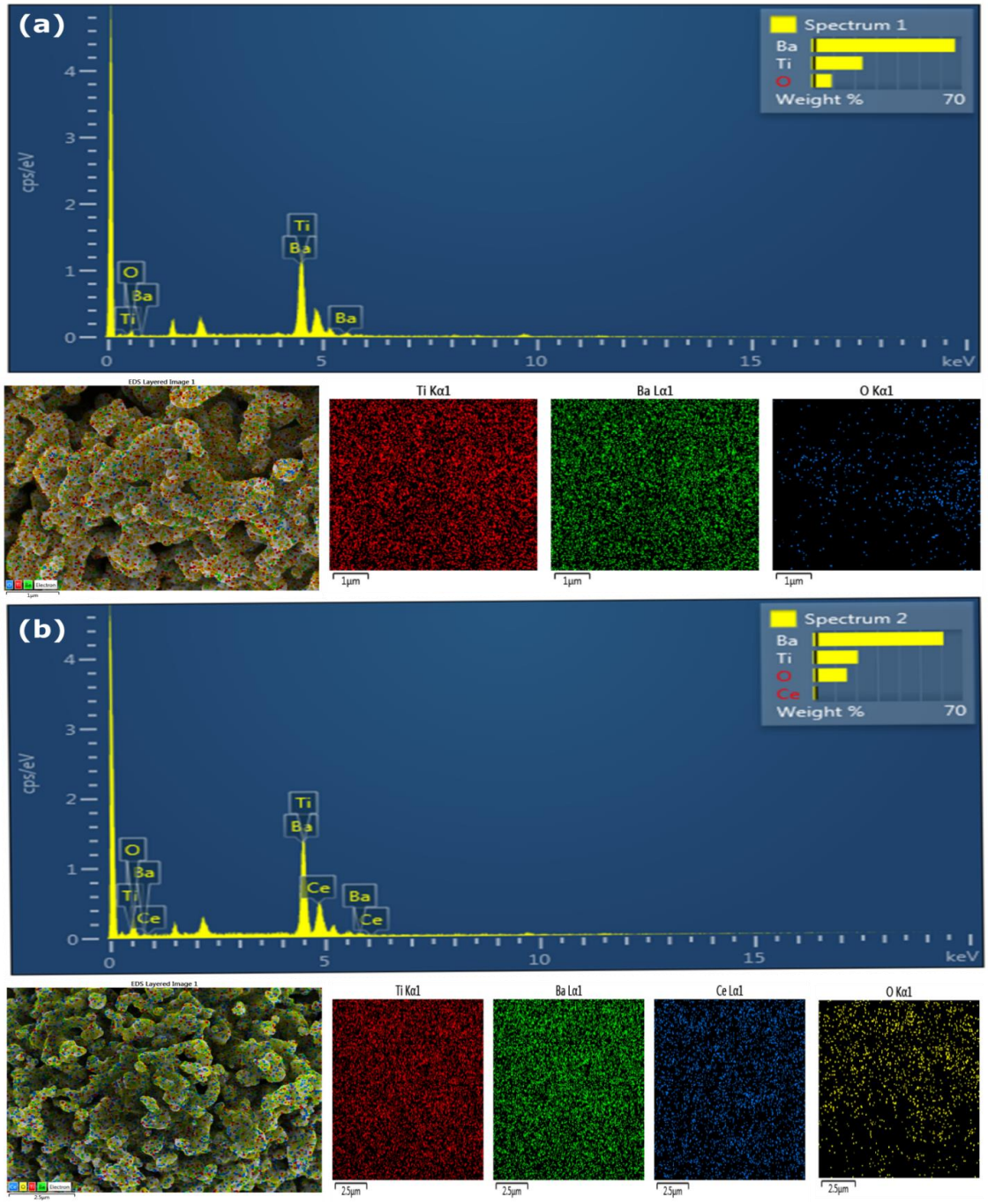
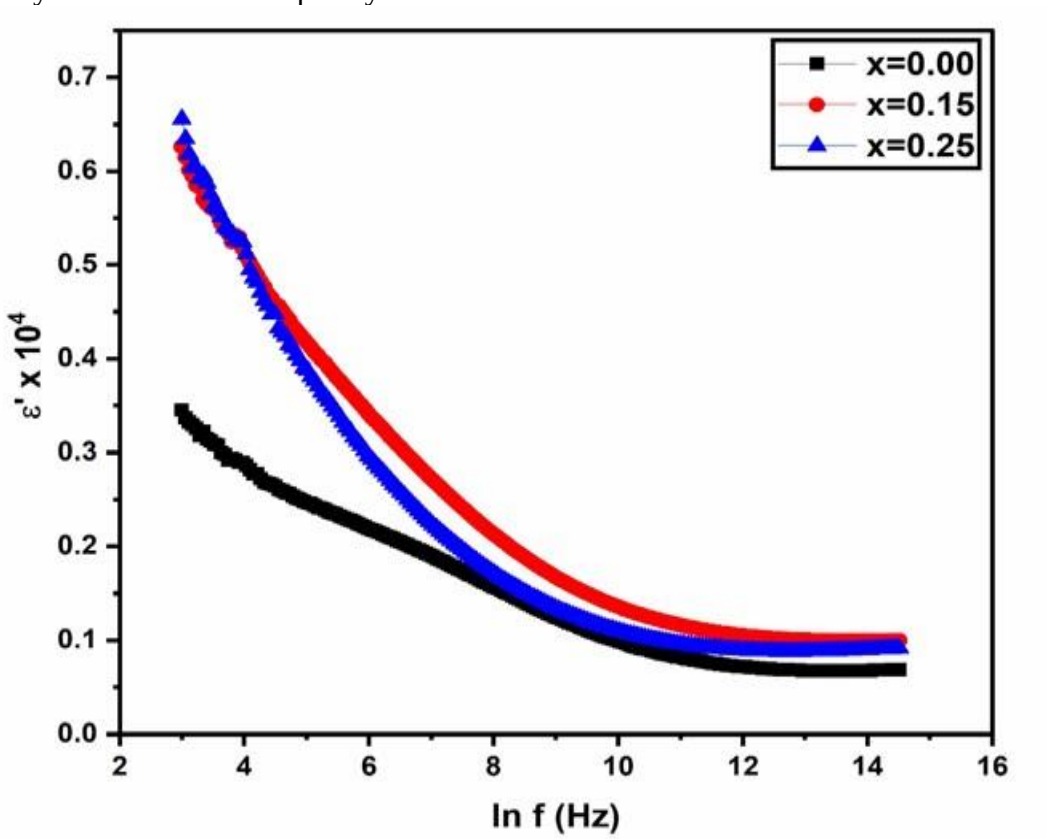


Fig. 4: EDX spectra and mapping of BaTi1-xCexO3 (x = 0.00 and 0.25)

3.4 Dielectric Analysis

The dielectric properties of Ce-doped $BaTiO_3$ ceramics were investigated by measuring the real part of the dielectric permittivity (ε′), dielectric loss tangent (tan δ), and AC conductivity as functions of frequency. These measurements provide insight into the polarization mechanisms, defect structure, and conduction behavior of the material, which are critical for MLCC applications.



Fig, 5: Room temperature Dielectric constant of $BaTi_{1-x}Ce_xO_3$ (x = 0.00, 0.15, and 0.25)

From Fig.5, it is clearly observed that the dielectric constant (ε′) increases with an increase in cerium (Ce) doping concentration, particularly at low frequencies. The highest recorded value of the dielectric constant, ε′ = 6700, was observed for the sample with x = 0.25 at a frequency of 30 Hz. This significant enhancement in dielectric response can be attributed to several interrelated factors.

Firstly, the substitution of Ce^{4+} ions at the Ti^{4+} sites within the perovskite structure leads to lattice expansion, as evidenced by the increase in unit cell volume reported in Table 1. This expansion enhances the polarizability of the lattice, thereby increasing the dielectric constant. Secondly, structural analysis using X-ray diffraction (XRD) reveals a transition from a tetragonal to a pseudo-cubic symmetry with increasing Ce content. This structural transformation tends to lower the Curie temperature closer to room temperature and broadens the temperature range over which high dielectric constant values are sustained. Such behavior is consistent with previous reports (Y.-M. Zhang et al., 2006; Ganguly et al., 2013), and it implies improved temperature stability in the dielectric performance of the material.

Additionally, at lower frequencies, the dielectric response is significantly influenced

by interfacial polarization, dipolar relaxation, and space charge accumulation. These polarization mechanisms become more pronounced in the Ce-doped samples due to the reduction in oxygen vacancies and the improvement in microstructural homogeneity. Studies by Beena & Jayanna (2019) and Mitic et al. (2010) support this observation, suggesting that Ce doping optimizes defect chemistry and charge distribution within the grains and at the grain boundaries.

Furthermore, Fourier Transform Infrared (FTIR) spectroscopy results, as shown in Figure 2, exhibit a blue shift in absorption peaks with increasing Ce concentration. This spectral shift is indicative of stronger Ce–O bonding and a corresponding increase in bond energy, which contributes to improved chemical and thermal stability. Such stability further reinforces the material's ability to sustain high dielectric constants (Kim et al., 2012; Kumari et al., 2015).

Finally, microstructural analysis using Field Emission Scanning Electron Microscopy (FESEM), presented in Figure 3, shows that Ce doping results in the formation of larger and more uniform grains. The reduction in grain boundary defects facilitates easier domain wall motion, which plays a crucial role in enhancing polarization behavior and thereby increasing the dielectric constant. This observation is consistent with previous findings by Feng et al. (2012) and Zhong et al. (2005), who reported similar correlations between grain size and dielectric performance.

In summary, the observed increase in ε′ with Ce doping is a synergistic outcome of lattice expansion, structural transitions, enhanced polarization mechanisms, stronger chemical bonding, and improved microstructural characteristics.

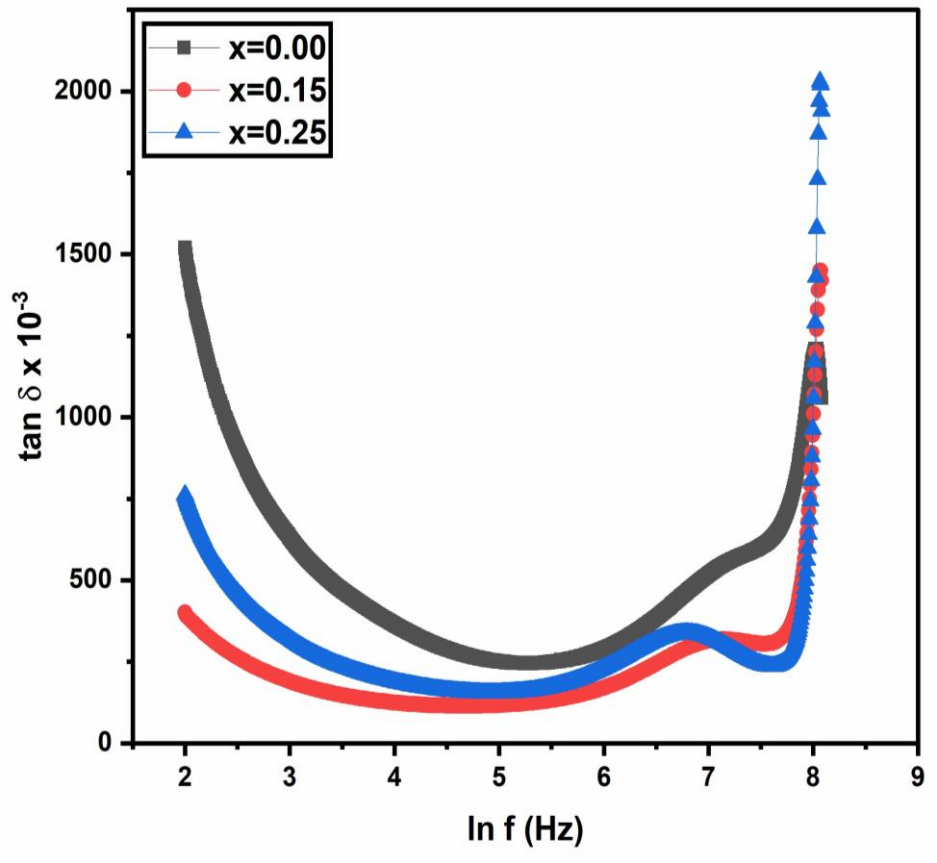
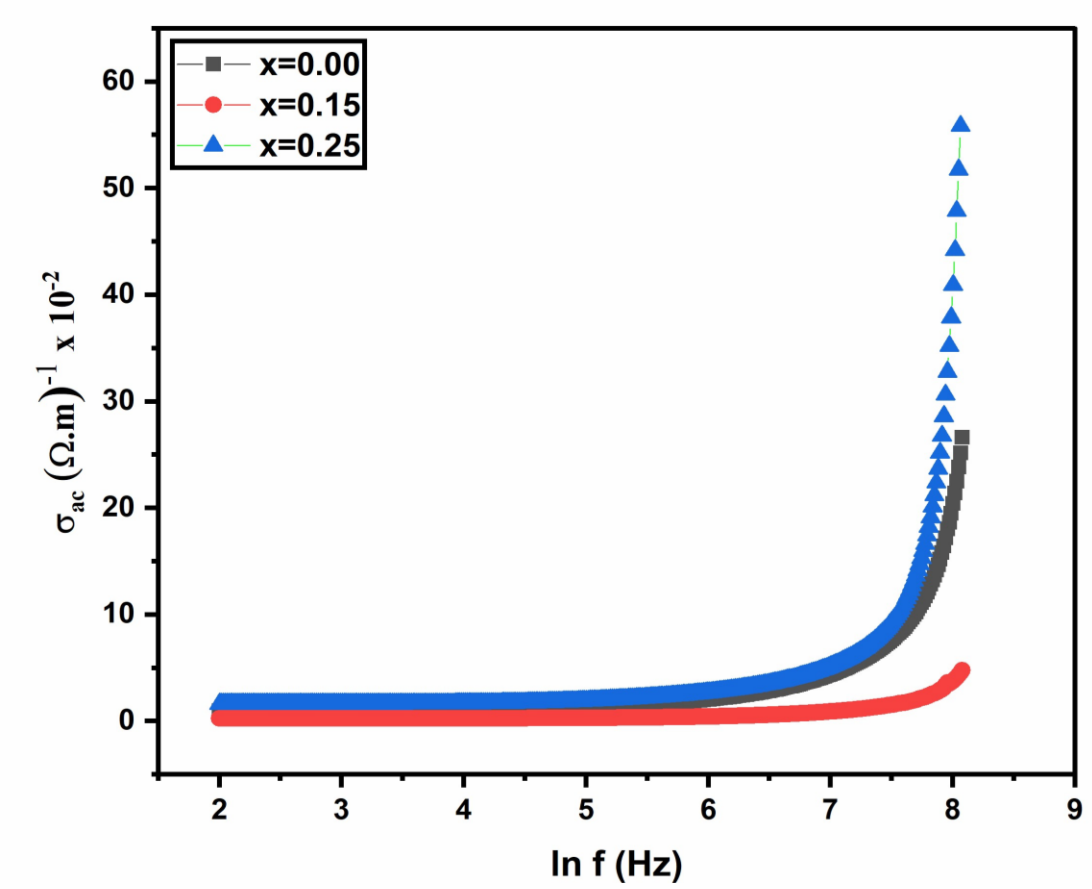


Fig., 6: Room temperature Dielectric loss tangent of BaTi1-xCexO3 (x = 0.00, 0.15, and 0.25).

Regarding dielectric loss (tan δ), Fig. 6 shows a decrease at low frequencies with Ce doping, suggesting lower leakage currents and fewer defect-induced conduction paths. This aligns with previous findings that Ce^{4+} substitution effectively compensates for B-site vacancies and reduces oxygen deficiency(Lu *et al.*, 2007; Petrović *et al.*, 2015). However, tan δ increases sharply at high frequencies, likely due to enhanced ionic mobility or electrode polarization effects.



Fig, 7: Room temperature AC conductivity of BaTi1-xCexO3 (x = 0.00, 0.15, and 0.25)

The alternating current (AC) conductivity measurements presented in Figure 7 reveal distinct frequency-dependent behavior characteristic of dielectric ceramics. At low frequencies, the conductivity exhibits a nearly frequency-independent trend. This behavior is typically associated with hopping conduction or band transport mechanisms, where localized charge carriers move between defect states or through narrow energy bands. As the frequency increases, the conductivity begins to rise more noticeably, which can be attributed to phenomena such as ionic relaxation or electrode polarization. These effects are common in dielectric materials where mobile ions respond to the alternating field but cannot follow rapid changes at higher frequencies. The observed increase in AC conductivity with frequency in the Ce-doped $BaTiO_3$ samples aligns well with previous studies (Beena & Jayanna, 2019) and supports the potential of these materials for high-frequency electronic applications.

Taken together, the dielectric and electrical behaviors observed in this study provide compelling evidence that Ce doping has a

multifaceted positive effect on $BaTiO_3$. It not only improves the structural and morphological characteristics of the ceramic matrix but also enhances its electrical properties. The combination of high dielectric constant, stable conductivity response, and structural integrity makes Ce-doped $BaTiO_3$ a strong candidate for use in advanced multilayer ceramic capacitors (MLCCs) and related high-performance electronic devices.

In summary, the incorporation of Ce^{4+} into the $BaTiO_3$ lattice improves the dielectric constant (ε') and overall electrical performance through several interconnected mechanisms. The substitution of Ce^{4+} for Ti^{4+} leads to a measurable expansion of the unit cell, increasing the material's polarizability. Structural analysis confirms that this doping induces a shift from the tetragonal to pseudo-cubic phase, effectively lowering the Curie temperature toward room temperature. This structural adjustment enables the material to maintain high dielectric values over a broader temperature range.

Moreover, Ce doping enhances polarization phenomena, particularly at low frequencies, by promoting the formation of defect dipoles and increasing space charge accumulation. FTIR spectral shifts indicate stronger Ce–O bonding, which contributes to improved lattice stability and facilitates ionic displacement. Microstructural examinations reveal that Ce inclusion promotes grain growth, resulting in larger and more uniform grains that reduce internal defects and improve domain wall mobility.

Finally, the doped system exhibits reduced oxygen vacancy concentration and leakage currents, indicating effective defect compensation. This not only stabilizes the dielectric behavior but also contributes to the reliability and longevity of the material under electrical stress. Altogether, these enhancements underscore the suitability of Ce-doped $BaTiO_3$ for next-generation capacitive devices, confirming its potential as a highly functional material for miniaturised and high-efficiency electronic components.

4.0 Conclusion

The study comprehensively investigated the structural, microstructural, and dielectric properties of Ce^{4+}-doped $BaTiO_3$ ceramics synthesized via the sol-gel auto-combustion method. X-ray diffraction analysis confirmed that increasing Ce content induces a transition from a tetragonal to a pseudo-cubic phase, accompanied by lattice expansion and an increase in unit cell volume, attributed to the substitution of larger Ce^{4+} ions at Ti^{4+} sites. FTIR spectroscopy revealed a blue shift in absorption peaks with higher Ce concentrations, indicating stronger Ce–O bonding and increased bond energy, which enhance the material's chemical and thermal stability. Microstructural analysis using FESEM showed that Ce doping leads to the formation of larger, more uniform grains, resulting in improved density, reduced defects, and enhanced homogeneity of the ceramic matrix. Dielectric measurements demonstrated a marked increase in the dielectric constant, reaching a maximum value of $\varepsilon' = 6700$ at 30 Hz for the $x = 0.25$ composition, alongside a reduction in dielectric loss at low frequencies. AC conductivity studies indicated frequency-independent behavior at low frequencies and a frequency-dependent increase at higher frequencies, consistent with multiple conduction mechanisms. These findings collectively establish that Ce doping significantly improves the dielectric, structural, and morphological characteristics of $BaTiO_3$, making it a strong candidate for advanced multilayer ceramic capacitor (MLCC) applications[123].

In conclusion, the incorporation of Ce^{4+} into the $BaTiO_3$ lattice enhances the material's polarizability, stabilizes its structure, and optimizes its dielectric performance through synergistic effects on lattice parameters, defect chemistry, and grain morphology. The observed improvements in dielectric constant,

reduced loss, and structural integrity confirm the suitability of Ce-doped $BaTiO_3$ for use in miniaturized and high-efficiency electronic components123.

Based on these results, it is recommended that further research explore the optimization of Ce doping levels and processing conditions to maximize performance for specific electronic applications. Additionally, investigating the long-term reliability and temperature stability of Ce-doped $BaTiO_3$ in device-relevant environments will be valuable for accelerating its adoption in next-generation capacitive devices and other high-performance electronic systems

Acknowledgement

The authors are grateful to the Materials Research Centre, Malaviya National Institute of Technology, Jaipur, India, for FESEM/EDX characterizations.

5.0 Reference

Alam, M. A., Zuga, L., & Pecht, M. G. (2012). Economics of rare earth elements in ceramic capacitors. *Ceramics International*, 38, 8, pp. 6091-6098.

Alshoaibi, A., Kanoun, M. B., Haq, B. U., AlFaify, S., & Goumri-Said, S. (2020). Ytterbium doping effects into the Ba and Ti sites of perovskite barium titanate: Electronic structures and optical properties. *Results in Physics, 18*, 103257. doi"10.1016/j.rinp.2020.103257

Arshad, M., Du, H., Javed, M. S., Maqsood, A., Ashraf, I., Hussain, S., Ma, W., & Ran, H. (2020). Fabrication, structure, and frequency-dependent electrical and dielectric properties of Sr-doped BaTiO3 ceramics. *Ceramics International*, 46, 2, pp. 2238-2246.

Beena, P., & Jayanna, H. (2019). Dielectric studies and AC conductivity of piezoelectric barium titanate ceramic polymer composites. *Polymers and Polymer Composites, 27*, 9, pp. 619-625.

Cernea, M., Monnereau, O., Llewellyn, P., Tortet, L., & Galassi, C. (2006). Sol–gel synthesis and characterization of Ce doped-BaTiO3. *Journal of the European Ceramic Society, 26, 15, pp.* 3241-3246.

Feng, H., Hou, J., Qu, Y., Shan, D., & Yao, G. (2012). Structure, dielectric and electrical properties of cerium doped barium zirconium titanate ceramics. *Journal of alloys and compounds, 512, 1, pp.* 12-16.

Ganguly, M., Rout, S., Sinha, T., Sharma, S., Park, H., Ahn, C., & Kim, I. (2013). Characterization and rietveld refinement of A-site deficient lanthanum doped barium titanate. *Journal of alloys and compounds, 579*, pp. 473-484.

Hai, C., Inukai, K., Takahashi, Y., Izu, N., Akamatsu, T., Itoh, T., & Shin, W. (2014). Surfactant-assisted synthesis of mono-dispersed cubic BaTiO3 nanoparticles. *Materials Research Bulletin*, 57, pp. 103-109.

Hossain, M. K., Rubel, M., Akbar, M. A., Ahmed, M. H., Haque, N., Rahman, M. F., Hossain, J., & Hossain, K. M. (2022). A review on recent applications and future prospects of rare earth oxides in corrosion and thermal barrier coatings, catalysts, tribological, and environmental sectors. *Ceramics International*, 48, 22, pp. 32588-32612.

Hwang, J. H., & Han, Y. H. (2001). Electrical properties of cerium-doped BaTiO3. *Journal of the American Ceramic Society, 84, 8, pp.* 1750-1754.

Ismail, F. A., Osman, R. A. M., & Idris, M. S. (2016). *Review on dielectric properties of rare earth doped barium titanate.* Paper presented at the AIP conference proceedings.

Itoh, J.-i., PARK, D.-C., OHASHI, N., SAKAGUCHI, I., YASHIMA, I., HANEDA, H., & TANAKA, J. (2002). Oxygen diffusion and defect chemistry in rare-earth-doped BaTiO3. *Journal of the Ceramic Society of Japan, 110, pp.* 495-500.

Joshi, N., Shrinet, V., & Pratap, A. (2014). Influence of metal doping on electrical properties of nano barium titanate. *Advanced Electrochemistry, 2, 1, pp.* 3-8.

Kim, D., Kim, J., Noh, T., Ryu, J., Kim, Y.-n., & Lee, H. (2012). Dielectric properties and temperature stability of $BaTiO_3$ co-doped La_2O_3 and Tm_2O_3. *Current Applied Physics, 12,* 3, pp. 952-956.

Kumari, Kumar, P., & Rai, R. (2015). Study the structural and dielectric properties of rare-earth La doped $(Ba_{1-x}La_x)(Ti_{0.815}Mn_{0.0025}Nb_{0.0025}Zr_{0.18})_{0.995}O_3$ ceramics. *Integrated Ferroelectrics,* 167, 1, pp. 24-34.

Kumari, A., & Ghosh, B. D. (2018). La doped barium titanate/polyimide nanocomposites: a study of the effect of La doping and investigation on thermal, mechanical and high dielectric properties. *Journal of Applied Polymer Science,* 135, 47, 46826, doi 10.1002/app.46826

Lu, D.-Y., KODA, T., & TODA, H. S. M. (2005). Structural and Dielectric Properties of Eu-Doped Barium Titanate Ceramics. *Journal of the Ceramic Society of Japan,* 113, 11, pp. 721-727.

Lu, D.-Y., Sun, X.-Y., & Toda, M. (2007). A novel high-k 'Y5V'barium titanate ceramics co-doped with lanthanum and cerium. *Journal of Physics and Chemistry of Solids,* 68, 4, pp. 650-664.

Mitic, V. V., Nikolic, Z. S., Pavlovic, V. B., Paunovic, V., Miljkovic, M., Jordovic, B., & Zivkovic, L. (2010). Influence of rare-earth dopants on barium titanate ceramics microstructure and corresponding electrical properties. *Journal of the American Ceramic Society,* 93, 1, pp. 132-137.

Petrović, M. V., Bobić, J., Grigalaitis, R., Ilic, N., Dzunuzovic, A., Jankauskaite, V., Banys, J., & Stojanović, B. D. (2015). Donor–acceptor joint effect in barium titanate systems. *Ceramics International,* 41, 9, pp. 11365-11371.

Sharma, H., Jindal, S., & Aggarwal, N. (2020). Impact of copper doping on perovskite structure ferroelectric ceramic. *Materials Today: Proceedings,* 33, pp. 1632-1636.

Tsur, Y., Hitomi, A., Scrymgeour, I., & Randall, C. A. (2001). *Relaxor-like diffuse phase transitions in BaTiO$_{3}$ thin films*. Japanese Journal of Applied Physics, *40*(1R), 255. https://doi.org/10.1143/JJAP.40.255

Zhang, K., Li, L., Wang, M., & Luo, W. (2020). Charge compensation in rare earth doped BaTiO3-based ceramics sintered in reducing atmosphere. *Ceramics International,* 46, 16, pp. 25881-25887.

Zhang, Y.-M., Sun, X.-Y., & LU, D.-y. (2006). Effects of cerium doping at Ti sites and europium doping at Ba sites on dielectric properties of BaTiO3 ceramics. *Chemical Research in Chinese Universities,* 22, 4, pp. 515-519.

Zhao, Z., Liang, X., Zhang, T., Hu, K., Li, S., & Zhang, Y. (2020). Effects of cerium doping on dielectric properties and defect mechanism of barium strontium titanate glass-ceramics. *Journal of the European Ceramic Society,* 40, 3, pp. 712-719.

Zhong, N., Xiang, P.-h., Sun, D.-z., & Dong, X.-l. (2005). Effect of rare earth additives on the microstructure and dielectric properties of 0.67 Pb (Mg1/3Nb2/3) O3–0.33 PbTiO3 ceramics. *Materials Science and Engineering: B,* 116, 2, pp. 140-145.

Declaration

Consent for publication

Not applicable

Availability of data

Data shall be made available on demand.

Competing interests

The authors declared no conflict of interest

Ethical Consideration

Not applicable

Funding

There is no source of external funding.

Authors' Contributions

Fatima Musa Lariski designed and performed the experiments, carried out the synthesis and characterization of the Ce-doped $BaTiO_3$ ceramics, analyzed the data, and drafted the manuscript. Hassan Abdulsalam supervised the research, contributed to data interpretation, provided critical revisions, and approved the final version of the manuscript for publication